Current Cardiology Reports (2021) 23: 134
https://doi.org/10.1007/s11886-021-01564-6

ECHOCARDIOGRAPHY (JM GARDIN AND AH WALLER, SECTION EDITORS)

Multimodality Imaging in Cardiac Amyloidosis

Gerard T. Giblin[1] · Sarah A. M. Cuddy[1,2]

Accepted: 13 April 2021 / Published online: 19 August 2021

Abstract

Purpose of Review Cardiac amyloidosis is an increasingly recognized condition with a growing range of targeted therapies, but diagnosis requires a high index of suspicion and multimodality imaging expertise. Early diagnosis remains key to improving quality of life and survival. This article reviews the multimodality imaging approach to the diagnosis, differentiation, and prognosis of cardiac amyloidosis.

Recent Findings Recent advances in multimodality cardiac imaging have allowed for earlier diagnosis of cardiac amyloidosis resulting in earlier initiation of life-saving therapy in cases of light chain amyloidosis and life-prolonging therapy in transthyretin amyloidosis.

Summary With these advances in multimodality imaging, it is important for cardiologists and cardiac imagers to be aware of the subtleties of early disease, the appropriate diagnostic approach as well as understanding the practicalities and pitfalls that are encountered with each modality.

Keywords Cardiac amyloidosis · Multimodality imaging · Echocardiography · Cardiac magnetic resonance · Nuclear scintigraphy

Introduction

Cardiac amyloidosis occurs due to progressive extracellular accumulation of abnormal misfolded insoluble protein fibril aggregates and is characterized by a restrictive cardiomyopathy. The two commonest forms of cardiac amyloidosis are light chain (AL) amyloidosis, a systemic disorder where the amyloid protein is derived from misfolded monoclonal immunoglobulin light chains, and transthyretin (ATTR) amyloidosis, which results from deposition of misfolded transthyretin protein produced in the liver. This may be either wild type (wtATTR) due to age-related transthyretin misfolding or hereditary (hATTR) due a point mutation in the transthyretin (TTR) gene transmitted in an autosomal dominant fashion with varying patterns of cardiac and neuropathic involvement. The most common variant in the USA is Val122Ile, found in approximately 3–4% of Black Americans [1]. Wild-type ATTR predominantly affects older males and has been found in 13% of older patients hospitalized with heart failure with preserved ejection fraction and left ventricular (LV) wall thickness > 12 mm [2].

A combination of transthoracic echocardiography with deformation techniques, cardiac magnetic resonance imaging, and cardiac scintigraphy with bone-avid single-photo emission computed tomography (SPECT) radiotracers forms the basis for a thorough diagnostic workup in a patient presenting with new heart failure and a suspicion for cardiac amyloidosis. Cardiac imaging may also allow accurate determination of the amyloid subtype without the need for additional invasive testing in ATTR amyloidosis [3••]. A suggested algorithm for the diagnosis and subtyping of cardiac amyloidosis is shown in Figure 1.

This article reviews the multimodality imaging approach to the diagnosis, differentiation, and prognosis of cardiac amyloidosis as well as its role in the evaluation of response to treatment.

This article is part of the Topical Collection on *Echocardiography*

✉ Sarah A. M. Cuddy
scuddy1@bwh.harvard.edu

[1] Cardiac Amyloidosis Program, Cardiovascular Division, Department of Medicine, Heart & Vascular Centre, Brigham and Women's Hospital and Harvard Medical School, 15 Francis St, Boston, MA 02115, USA

[2] CV Imaging Program, Cardiovascular Division and Department of Radiology, Brigham and Women's Hospital, Boston, USA

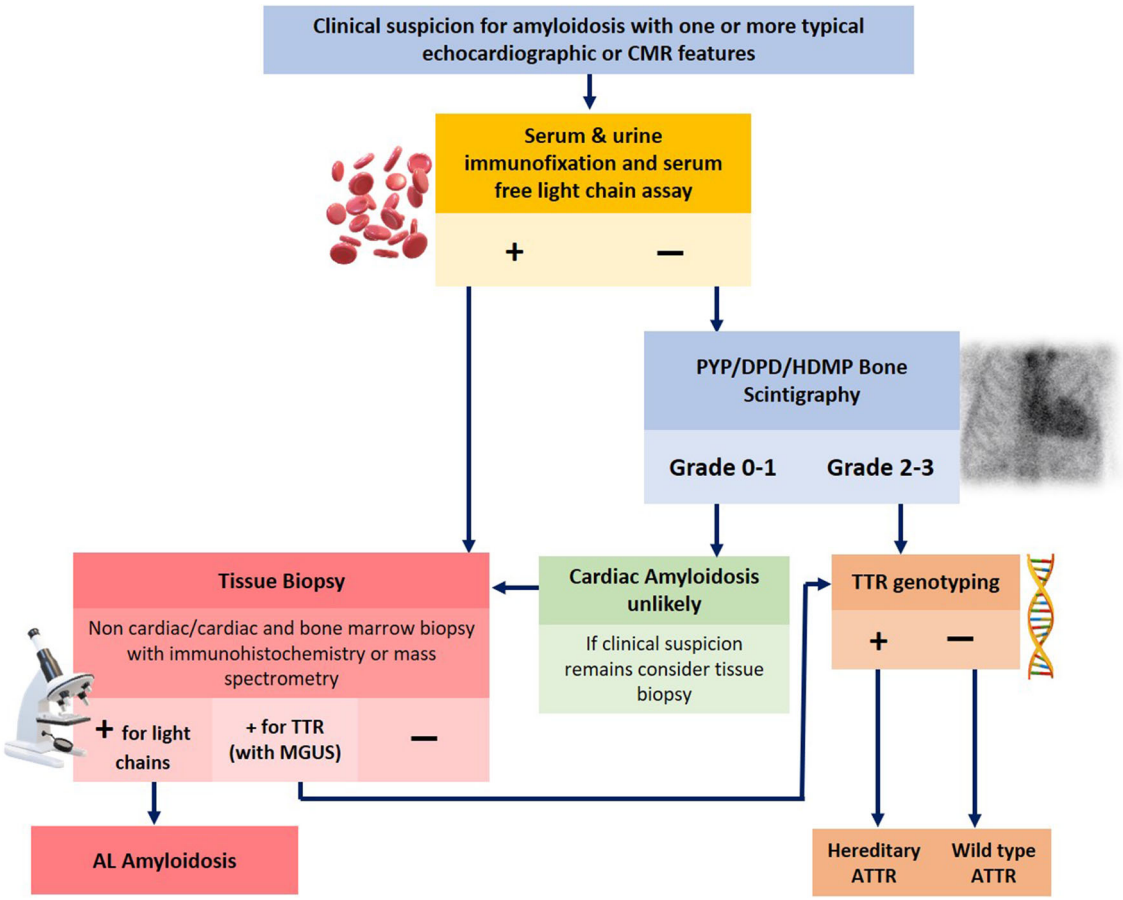

Figure 1 Suggested algorithm for the diagnosis of cardiac amyloidosis.

Echocardiography

Echocardiography is usually the first-line imaging investigation that patients presenting with heart failure or suspected cardiac amyloidosis will undergo and is commonly the initial modality that raises suspicion for cardiac amyloidosis based on morphological and functional changes due to amyloid fibril infiltration. The typical findings are listed in Table 1. This is an extensive list and not all features need to be present to raise the suspicion of amyloid infiltration.

Diagnosis

Many of the classical findings are not specific for cardiac amyloidosis. The granular, speckled pattern appearance of the infiltrated myocardium is also recognized in advanced chronic kidney disease and other infiltrative cardiomyopathies and may be confounded by newer harmonic imaging (Figure 2, panel A) [4]. Similarly, in the early stages of infiltration, mildly increased LV wall thickness can be difficult to distinguish from other causes such as hypertensive heart disease or other hypertrophic cardiomyopathy phenotypes. Wall thickening can be asymmetric and LV outflow tract obstruction is occasionally seen; 1% of patients undergoing surgical myectomy for presumed hypertrophic cardiomyopathy had amyloid deposition on pathology (Figure 2, panel B) [5]. The associated presence of interatrial septal thickening or increased RV wall thickness is strongly suggestive of an infiltrative cardiomyopathy as this is uncommonly seen in association with true LV hypertrophy [6]. Small circumferential pericardial effusions related to increased filling pressures are often seen and when present are associated with worse prognosis [7].

While it is not possible on echocardiography alone to reliably distinguish between AL and ATTR subtypes, several studies have looked at features that are more suggestive of one type. Mean wall thickness was greater in wild-type ATTR than in AL or hereditary ATTR (17 mm, 15 mm, and 15 mm, respectively) in a study of 172 subjects [6]. There was a similar pattern in mass index between the subtypes. Wall thickness correlated with worsening LV function regardless of the subtype. Unlike in AL amyloid, where the pattern of LV wall thickening is most often symmetrical, asymmetric septal wall thickening is the commonest pattern found in 79% patients with ATTR cardiac amyloid in one series (70% sigmoid septal, 30% reverse septal contour) [8].

Table 1 Echocardiographic findings in cardiac amyloidosis

Morphological	*Functional*
• Small LV cavity size • Increased LV wall thickness (> 1.2 cm) [60] • Increased relative LV wall thickness (ratio of QRS voltage to LV wall thickness) [61] • Increased myocardial echogenicity ("speckling") • Increased RV wall thickness • Atrial dilatation • Valvular thickening • Interatrial septal thickening • Pericardial effusion	• Reduced LV stroke volume index despite normal or near-normal ejection fraction • Reduced longitudinal function • Diastolic dysfunction (high E/A ratio > 1.5, E/e' > 15, deceleration time < 150 ms) • Reduced LV tissue Doppler velocities (e', a', and S' < 5 cm/s) • LV systolic dysfunction in advanced disease • Reduced LV global longitudinal strain • Preserved apical longitudinal strain relative to reduced basal and mid LV strain ("cherry-on-top" pattern on bullseye strain plot) • Increased estimated pulmonary pressures • Paradoxical low-flow low-gradient aortic stenosis • Dynamic LV outflow tract obstruction [5, 62] (Figure 2, panel B) • Abnormal left atrial strain

Amyloid infiltration is not limited to the ventricular myocardium; the atria are also commonly involved resulting in the classical marked biatrial dilatation pattern, compounded by the elevated ventricular filling pressures that accompany the diastolic dysfunction characteristic of cardiac amyloidosis. Reduced or even absent transmitral Doppler A wave velocities are often seen in those with cardiac amyloidosis despite sinus rhythm, reflecting atrial amyloid infiltration and reduced contractile function. This can often be accompanied by the presence of atrial thrombus despite sinus rhythm. A transmitral *A* wave velocity of < 30 cm/s in the presence of sinus rhythm in patients with AL amyloidosis has previously been shown to be associated with the presence of intracardiac thrombi [9]. Left atrial strain is also frequently reduced in patients with cardiac amyloidosis compared to normal controls [10].

Transmitral and tissue Doppler will usually show diastolic dysfunction in cardiac amyloidosis. This may be on a spectrum from impaired relaxation to a restrictive filling pattern characterized by a shortened deceleration time on transmitral pulse wave Doppler and reduced tissue Doppler velocities in the LV myocardium (Figure 2, panel D). The ratio of E/e' may also be elevated and exceeds 15 consistent with increased LV filling pressures [11].

Often, the typical constellation of findings is present only in the more advanced stages of the disease, which may limit the specificity of echocardiography in earlier or subclinical disease. LV systolic function as measured by ejection fraction will usually be preserved until relatively late in the disease course, and therefore, markers of longitudinal function or more sensitive echocardiographic markers of subtle or subclinical dysfunction such as strain must be used to detect cardiac involvement before the onset of a heart failure syndrome [12, 13•]. A study by Knight et al. of 322 subjects with cardiac amyloidosis undergoing echocardiography and cardiovascular magnetic resonance imaging (CMR) found that global longitudinal strain and E/e' were the echocardiographic parameters with the highest probability of being abnormal at low cardiac amyloid burden as defined by the extracellular volume (ECV) at CMR, while decreasing biventricular ejection fraction and increasing indexed atrial areas were more likely to be abnormal at high amyloid burden [13•].

Cardiac amyloidosis has a characteristic pattern of global longitudinal strain (GLS) on speckle tracking echocardiography with severe impairment of the basal and mid segments with relative apical sparing, producing a classical "cherry-on-top" bullseye plot (Figure 2, panel C). This was quantified by Phelan et al. by calculating the relative apical longitudinal strain (ratio of apical longitudinal strain/sum of base and mid longitudinal strain); they found that a ratio > 1.0 was 93% sensitive and 82% specific at differentiating cardiac amyloidosis from other causes of increased LV wall thickness [14]. The exact pathological mechanism underlying this differential strain pattern is currently unknown. In another study evaluating the utility of strain for diagnosis of amyloidosis, a systolic septal longitudinal base-apex strain gradient (septal apical to basal longitudinal strain ratio > 2.1) combined with a shortened diastolic deceleration time of early filling (< 200 ms) had a sensitivity of 88%, specificity of 85%, and negative predictive value of 96% at differentiating cardiac amyloidosis from other causes of concentric left ventricular hypertrophy (LVH) and preserved ejection fraction (EF) [15]. Deformation-based echo techniques incorporating GLS and relative apical sparing have been shown to outperform conventional echo parameters such as EF or E/e' for the diagnosis of both ATTR and AL cardiac amyloid when compared to hypertensive and hypertrophic cardiomyopathy controls [16•].

Prognosis

In addition to its central role in the diagnosis of cardiac amyloidosis, a number of echocardiographic parameters have been shown to be independent predictors of prognosis. LV wall thickness > 15 mm, RV dysfunction, and hypertrophy are associated with poorer prognosis [17, 18]. Markers of diastolic

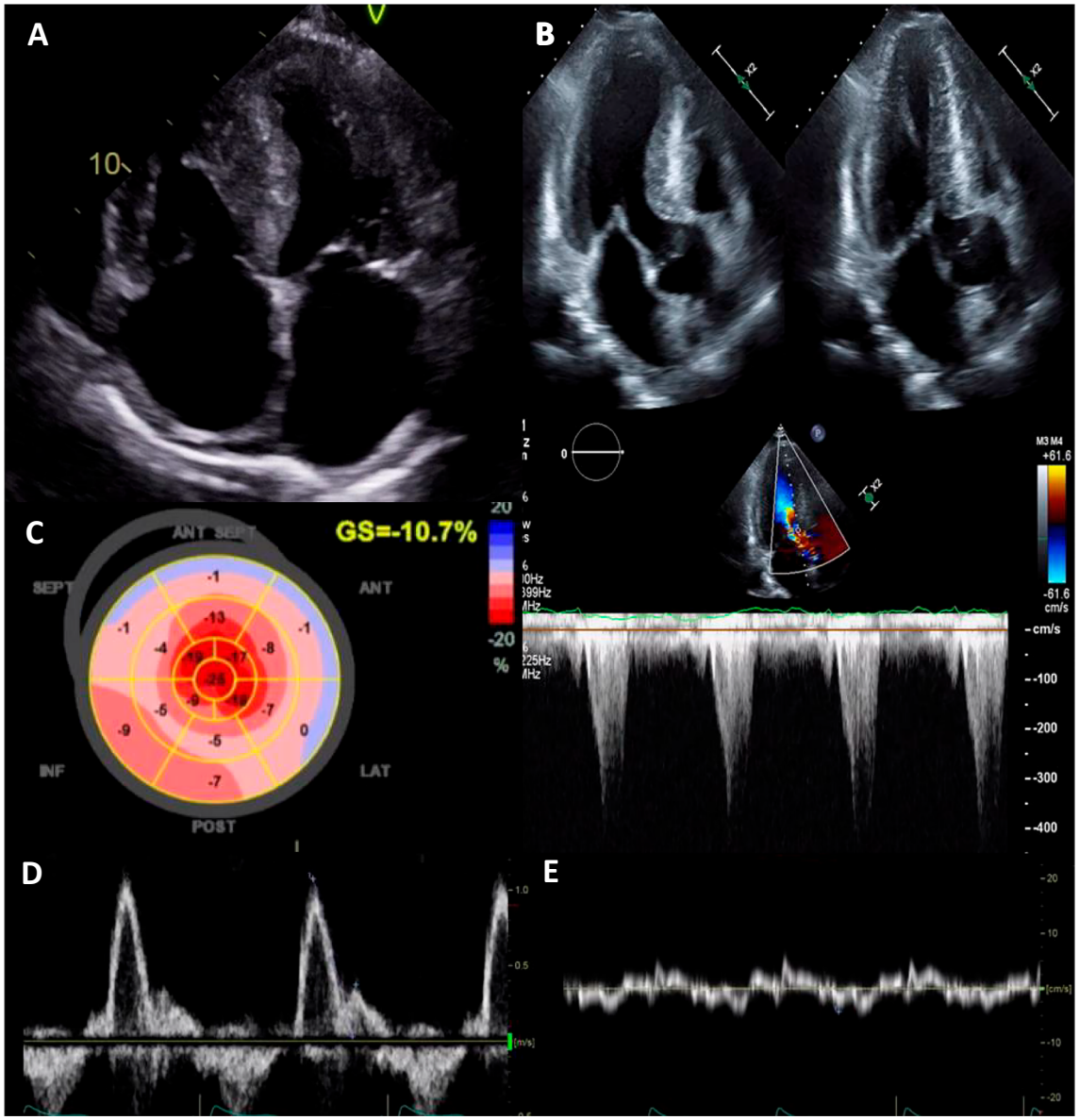

Figure 2 Echocardiographic features of cardiac amyloidosis**. A** Apical 4 chamber view showing a classical pattern of severe biventricular hypertrophy with a specked myocardial appearance, severe biatrial dilatation, and a small pericardial effusion. **B** Systolic anterior motion of the mitral valve leaflets and LVOT obstruction with a characteristic dynamic outflow tract obstruction continuous wave Doppler profile in a patient with light chain cardiac amyloidosis. **C** Speckle tracking echocardiography showing the characteristic longitudinal strain pattern with severe impairment of the basal and mid segments with relative apical sparing in a patient with wild-type ATTR amyloidosis. **D** Transmitral pulse wave Doppler showing restrictive mitral inflow filling pattern with an *E*/*A* ratio of 2.86. **E** reduced tissue Doppler velocities (*e*′, *a*′, and *s*′ < 5 m/s) at the lateral mitral annulus with an *E*/*e*′ ratio 25 in a patient with AL amyloidosis.

dysfunction such as left atrial enlargement, shortened deceleration time (< 150 ms), and an increased early diastolic filling velocity to atrial filling velocity ratio (*E*/*A*) predict cardiac mortality [19, 20]. In AL amyloidosis, GLS ≥ 15% provided incremental prognostic value over current staging parameters such as troponin and NTproBNP [21]. Further work is needed in risk prediction using echo parameters, especially in ATTR cardiac amyloidosis; tracking response to therapy will also become important as the number of therapies available expands, to aid clinical decision-making.

CMR

Magnetic resonance imaging plays an integral role in the diagnosis of cardiac amyloidosis given its ability to provide high spatial resolution, three-dimensional structural and functional imaging, and quantifiable tissue characterization with T1 and T2 mapping and extracellular volume calculation, useful for both diagnosis and the potential to track treatment response. It can overcome some of the limitations of echocardiography such as poor acoustic windows with larger body habitus.

Depending on geographic location, availability may be limited by cost and technical expertise.

The characteristic morphological features of amyloidosis seen with CMR are similar to the morphological findings on echocardiography (Table 1). However, CMR allows a more accurate, three-dimensional assessment of ventricular volumes, function, and mass (Figure 3, panel A).

Post-contrast Imaging

One of the main strengths of CMR imaging is the ability to characterize tissue composition, which is augmented with the use of gadolinium-based contrast agents. Gadolinium is an extracellular agent which cannot cross the intact membrane of the cardiomyocyte and accumulates in the interstitium infiltrated by amyloid fibrils, which is greatly expanded compared to normal myocardium. Early gadolinium enhancement images can be acquired in the first 2–3 min following administration of a gadolinium-based contrast agent, usually with an inversion recovery prepared T1 gradient echo sequence with a manually selected short inversion time or phase-sensitive-inversion recovery sequence. This sequence is useful for visualizing avascular structures such as ventricular or atrial thrombi, but not routinely part of our amyloidosis CMR protocol.

Cardiac amyloidosis has a characteristic pattern on late gadolinium imaging (Figure 3, panel B), yet often the first indication of amyloid infiltration can be abnormal gadolinium kinetics seen on post-gadolinium T1 inversion recovery imaging. The blood pool normally nulls before the myocardium; however, in cardiac amyloidosis, this is simultaneous or reversed, with nulling of the myocardium prior to the ventricular blood pool, due to a more rapid washout of gadolinium from the blood pool and has been shown to correlate with a higher extracellular volume [22]. This can be demonstrated on an inversion time scout over a range of increasing inversion times performed approximately 5 min after gadolinium administration with high sensitivity and specificity for the diagnosis of amyloidosis while being a strong predictor of mortality [23].

Conventional magnitude only late gadolinium imaging requires an operator-determined inversion time in order to appropriately null the myocardium, which is often difficult to

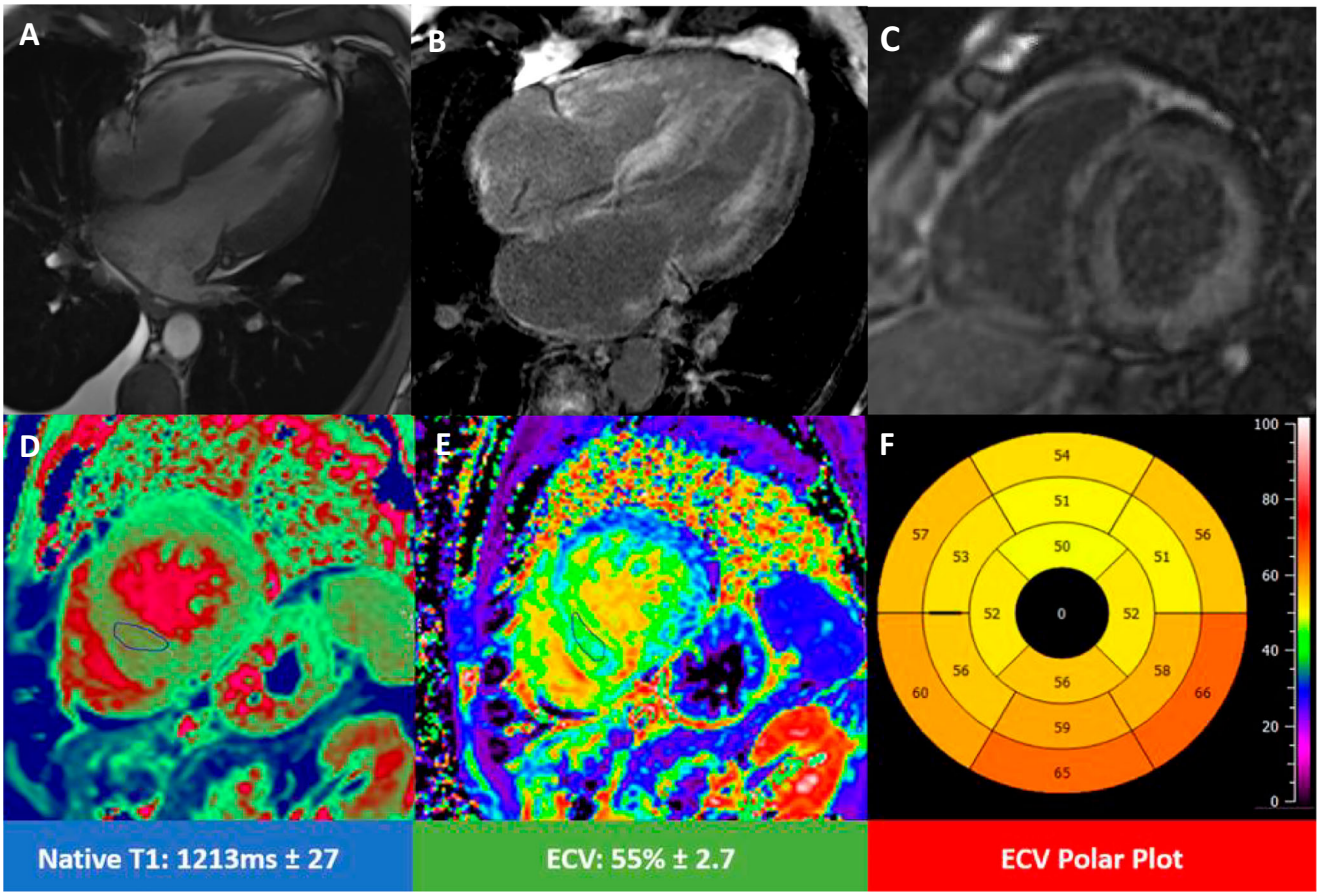

Figure 3 CMR imaging in cardiac amyloidosis. **A** Four-chamber cine imaging depicting concentric LVH with apical sparing and small pleural and pericardial effusions in a patient with wtATTR. **B**, **C** Four-chamber and short-axis late gadolinium imaging showing biatrial enhancement and the characteristic global circumferential subendocardial LV and RV enhancement with a basal-apical gradient and dark blood pool in a patient with AL amyloidosis. **D**, **E**, **F** Mid ventricular native T1 map, ECV map, and polar plot in a patient with wtATTR cardiac amyloidosis showing increased values.

achieve in cardiac amyloidosis due to abnormal kinetics from increased retention of gadolinium in the expanded interstitial space compared to normal myocardium. Some standard CMR protocols perform this sequence 10-min post-gadolinium administration, but at this point, the low levels of gadolinium in the blood pool can make image interpretation challenging. The use of a phase-sensitive inversion recovery (PSIR) sequence is superior at appropriately nulling the myocardium [24]. Enhancement occurs in areas of increased extracellular space due to higher regional gadolinium concentration and slower washout kinetics than in normal myocardium [25]. The typical enhancement pattern is on a spectrum from none to globally subendocardial to globally transmural with a darkened blood pool [22, 26] (Figure 3, panels B and C). A transmural LGE pattern has been shown to be an independent predictor of mortality (hazard ratio 4.1, 95% confidence interval 1.3–13.1; $P < 0.05$) [24]. It had been suggested that different patterns of LGE can differentiate between ATTR and AL, with a transmural pattern more likely in ATTR type [27]. However, that is not our clinical experience and those findings may reflect the longer duration of disease burden in ATTR compared to AL amyloid or LGE imaging prior to the utilization of PSIR LGE imaging. LGE can also detect early cardiac amyloidosis in those without typical echocardiographic features. In a prospective study of 45 subjects with AL amyloidosis with or without cardiac involvement who underwent echocardiography, CMR and 18F-florbetapir positron emission tomography/computed tomography (PET/CT) demonstrated that 20% of the cohort with active AL amyloidosis without cardiac involvement by conventional criteria had evidence of cardiac amyloid deposition by late gadolinium enhancement and elevated ECV [28].

Exertional anginal symptoms are common in cardiac AL amyloidosis, and it is known from PET perfusion imaging that coronary microvascular dysfunction is highly prevalent in cardiac amyloidosis in the absence of epicardial coronary disease with reduced rest and stress myocardial blood flow [29]. A global subendocardial resting perfusion defect can be seen on CMR perfusion imaging.

Native Tissue Characterization (T1 and T2 mapping)

Native T1 mapping measures the intrinsic signal from a composite of the intracellular and interstitial components of the myocardium before administration of gadolinium contrast and allows detection of interstitial expansion due to myocardial edema and fibrosis (Figure 3, panel D) [30, 31]. Native myocardial T1 is elevated in cardiac amyloidosis, with higher values in amyloidosis compared with subjects with hypertrophic cardiomyopathy and normal controls [32]. Native T1 mapping may also allow earlier detection of amyloid infiltration, particularly in AL amyloid, before the appearance of conventional late gadolinium enhancement [33]. Increased native T1 values have been shown to be adversely associated with survival in both AL and ATTR amyloid [34, 35•].

One of the disadvantages of native parametric mapping with CMR is the lack of universal reference values as values are affected by factors such as magnet strength, vendor, the type of sequence used (MOLLI or ShMOLLI), and individual magnet properties and inhomogeneities. Therefore, it is recommended that each individual magnet has its normal reference range determined and benchmarked against published ranges [36].

Extracellular Volume

Integration of post-gadolinium T1 mapping with native T1 mapping allows characterization and quantification of the extracellular compartment of the myocardium or ECV (Figure 3, panels E and F). ECV may be used as a measure of amyloid burden and has been shown to correlate with functional performance by 6-min walk test and NT proBNP [37]. A contemporaneous hematocrit value is required and post-contrast T1 mapping performed 10–30-min post-gadolinium administration [36]. While ECV is highest in myocardial segments with visualized LGE in cardiac amyloidosis, it has been shown to be elevated in segments without LGE and therefore potentially detect amyloid infiltration at an earlier stage [38]. Increased ECV values have greater prognostic ability compared to native T1 values in ATTR amyloid and values over 45% are associated with reduced survival in AL amyloid [34, 35•].

T2 Mapping

T2 mapping allows for the detection and quantification of myocardial edema. In a single-center study of subjects with amyloidosis, T2 relaxation times were highest in untreated AL patients (56.6 ms) followed by treated AL (53.6 ms) and lowest in ATTR (48.9 ms). However, in this study, there was no correlation between edema on biopsy and myocardial T2. Increased myocardial T2 was an independent predictor of mortality in AL amyloid, but not ATTR [39]. This may be explained by the relatively greater toxicity of light chain amyloid to the myocardium than transthyretin fibrils.

Monitoring Response to Treatment

As we have described, several CMR parameters have prognostic value; several studies have shown that the LGE pattern can serve as an independent predictor of prognosis and a study of patients with ATTR showed ECV remained independently predictive after adjustment for age, N-terminal pro B-type natriuretic peptide, left ventricular ejection fraction, *E*/*e*′, left ventricular mass index, DPD grade, and late gadolinium enhancement [35•]. There is now a focus on tracking response to therapy using CMR. Studies to date have either been small

and retrospective or sub-group analyses of patients with hATTR. LGE regression and decrease in ECV have been seen in these smaller cohorts; more prospective longitudinal data is needed before this is used in clinical decision-making [40•, 41].

Radionuclide Imaging

Bone Tracer Cardiac Scintigraphy

Nuclear imaging in the form of radiolabelled phosphate-derived bone tracer cardiac scintigraphy has emerged as a highly sensitive and specific test for the diagnosis of cardiac transthyretin (ATTR) amyloidosis without the need for endomyocardial tissue sampling [3••]. While its role is incremental to functional and structural data provided by echocardiography and CMR, it has unique value in the differentiation between immunoglobulin light chain and TTR amyloid subtypes. The exact mechanism accounting for this preferential uptake in ATTR amyloidosis is not entirely understood. It has been postulated that it may relate to the binding of these phosphate-derived tracers to the relatively high calcium content of TTR fibrils compared to AL fibrils [42]. The three main tracers used internationally are 99mTc-labeled pyrophosphate (PYP), 99mTc-labeled hydroxymethylene diphosphonate (HMDP), and 99m technetium (Tc)-labeled 3,3-diphosphono-1,2-propanodicarboxylic acid (DPD). The choice of tracer depends on local availability, and to date, apart from single-case reports or case series, no direct head-to-head comparison has been performed to demonstrate the superior diagnostic ability of one tracer over another. In general, the same principles apply to all 3 tracers.

Conventionally, myocardial uptake can be quantitatively assessed at 1 or 3 h using the heart/contralateral ratio or at semi-quantitatively using the visual Perugini method. Tracer uptake at 3 h post-injection is compared between the myocardium and bone uptake and graded visually according to the semi-quantitative system developed by Perugini (Figure 4, panel A). Grade 0 represents no myocardial tracer uptake; grade 1 is when myocardial uptake is present but less than rib uptake; grade 2 where myocardial and rib tracer uptake are similar; and grade 3 correlates with diffuse intense myocardial greater than rib. Grade 2–3 uptake is strongly suggestive for ATTR amyloidosis [43]. Grade 1 uptake is equivocal and may represent either early ATTR amyloid or AL amyloid [44••]. Similar scoring systems have been developed to incorporate soft tissue uptake [45].

A seminal multicenter study by Gilmore et al. showed grade 2–3 cardiac uptake on bone scintigraphy in patients with a suggestive echocardiogram or CMR and absent monoclonal protein in urine or serum using electrophoresis with immunofixation, and a serum-free light chain assay has a specificity and a positive predictive value of 100% for the diagnosis of transthyretin cardiac amyloidosis [3••]. Any myocardial uptake (grade 1, 2, or 3) was > 99% sensitive for ATTR amyloid but less specific at 68%, with the lower specificity almost entirely due to uptake seen in patients with AL amyloidosis and cardiac apolipoprotein A–I amyloidosis. This highlights the need for adjunctive screening for a monoclonal protein in parallel with imaging for definitive exclusion of AL amyloid. This forms the basis for the expert consensus-recommended diagnostic algorithm for cardiac amyloidosis without the need for invasive histological confirmation. In the presence of a monoclonal protein, histological confirmation is required to accurately determine the amyloid subtype [3••, 45].

The ratio of heart to contralateral (H/CL) uptake is another diagnostic parameter utilized, where uptake in a region of interest over the myocardium on anterior planar images is corrected for uptake in a region of interest in the contralateral chest at 1 h after tracer administration (Figure 4, panel B). Using mean counts, a heart-contralateral ratio > 1.5 for 99Tc-PYP has been shown to distinguish ATTR from AL cardiac amyloidosis [46]. Care must be taken to avoid sternal overlap and maximize myocardial coverage without including adjacent lung. Use of the Perugini visual score and H/CL ratio has recently been found to be more sensitive but less specific when measured at 1 h than at 3 h [47]. With the increased use of technetium-labeled bone-avid cardiac scintigraphy, there has been an increase in misinterpretation of these scans, often due to inadequate image acquisition. A frequent reason for false positive results on planar imaging is persistent blood pool uptake [48•]. It is recommended that SPECT imaging should always be obtained in those patients who have positive or equivocal myocardial uptake on planar imaging to allow differentiation of myocardial uptake from background blood pool or adjacent bone uptake and thereby minimize the chance of a false positive scan (Figure 4, panel C) [44••], ideally with computed tomography (CT) for tissue attenuation, if available. This allows minimization of the possibility of a false positive result due to the ability of infarcted myocardium to take up these tracers with SPECT permitting simultaneous visualization of infarcted myocardium in a typical coronary territory [49].

Certain variants of hereditary ATTR amyloidosis such as early-onset V30M and Se77Tyr have been associated with false negative scintigraphy despite the presence of cardiac amyloid infiltration histologically, and amyloid binding PET radiotracers may be more sensitive when these mutations are suspected [8, 50, 51]; hence, diagnostic algorithms emphasize that tissue biopsy should be considered if a high index of suspicion remains despite negative cardiac scintigraphy. As well as non-ATTR forms of cardiac amyloidosis, hydroxychloroquine cardiotoxicity has also been shown to replicate the typical longitudinal strain pattern found in cardiac amyloid and cause false positive results on scintigraphy [52].

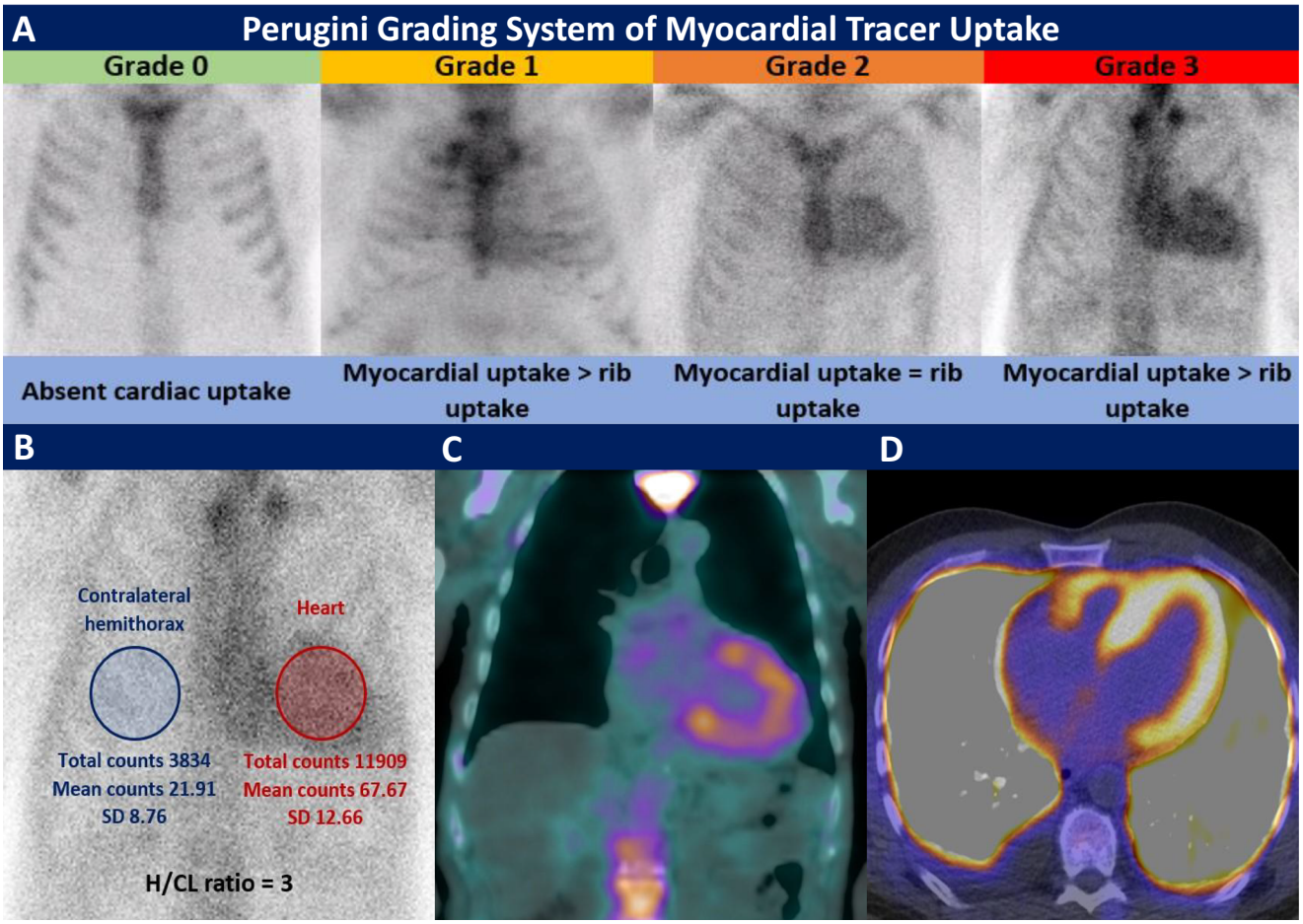

Figure 4 Nuclear imaging in cardiac amyloidosis. **A** Qualitative Perugini grading system of myocardial uptake of 99mTc-labeled pyrophosphate tracer on planar imaging at 3 h. **B** Quantitative assessment of myocardial uptake of Tc99-PYP at 1-h post-tracer administration using the heart-contralateral ratio. **C** Fused SPECT/Planar imaging in a patient with Perugini grade 3 uptake helps distinguish myocardial uptake from blood pool activity. **D** 18F-florbetapir positron emission tomography showing diffuse biventricular uptake in a patient with AL amyloidosis and pulmonary uptake.

Currently, bone scintigraphy is recommended as the imaging test of choice in addition to serum and urine testing for a monoclonal protein in patients suspected to have amyloidosis either clinically or with suggestive echo or CMR findings [3••]. Interest has grown in the diagnostic potential of these tracers in screening for cardiac amyloidosis in certain patient populations known to have a higher prevalence of ATTR amyloid such as carpal tunnel syndrome (10%), heart failure with preserved ejection fraction, and LVH (13%) or aortic stenosis requiring TAVR (13%) [2, 53•, 54].

Amyloid Binding PET Radiotracers

Thioflavin-analogue PET tracers have been found to bind to amyloid fibrils and have been used to image both cardiac and systemic amyloidosis. The main compounds under investigation at present are 18F-florbetapir, 18F-florbetaben, and 11C-labeled Pittsburgh Compound-B [55–57] (Figure 4, panel D). These tracers bind to the beta-pleat of the amyloid fibril and can be used to visualize both AL and ATTR amyloid [58]. For now, they remain investigational but may offer incremental benefit beyond currently used imaging techniques for early diagnosis and monitoring response to amyloid-specific therapies.

Monitoring Response to Treatment

To date, there is no evidence available or consensus on the use of serial bone scintigraphy once a diagnosis has been established or in the assessment of response to amyloid-specific therapy [59].

Conclusion

Cardiac amyloidosis has several classical features across echo and CMR; it is essential for a cardiac imager to be able to recognize these features and raise the possibility of cardiac

amyloidosis. Technetium-labeled cardiac scintigraphy has allowed for the non-invasive diagnosis of ATTR cardiac amyloidosis in the absence of a monoclonal gammopathy, enabling us to understand more about the prevalence of this disease. With advances in multimodality imaging, it is important for cardiologists and cardiac imagers to be aware of the subtleties of early disease, to allow earlier initiation of life-saving therapy in the cases of AL and life-prolonging therapy in ATTR, as well as understanding the pitfalls that are encountered with each modality.

Declarations

Conflict of Interest GG: No conflicts of interest to declare.
SC: Investigator-initiated research grant from Pfizer.

Human and Animal Rights and Informed Consent This article does not contain any studies with human or animal subjects performed by any of the authors.

References

Papers of particular interest, published recently, have been highlighted as:
• Of importance
•• Of major importance

1. Jacobson DR, Pastore RD, Yaghoubian R, Kane I, Gallo G, Buck FS, et al. Variant-sequence transthyretin (isoleucine 122) in late-onset cardiac amyloidosis in black Americans. N Engl J Med. 1997;336(7):466–73.
2. Gonzalez-Lopez E, Gallego-Delgado M, Guzzo-Merello G, de Haro-Del Moral FJ, Cobo-Marcos M, Robles C, et al. Wild-type transthyretin amyloidosis as a cause of heart failure with preserved ejection fraction. Eur Heart J. 2015;36(38):2585–94.
3.•• Gillmore JD, Maurer MS, Falk RH, Merlini G, Damy T, Dispenzieri A, et al. Nonbiopsy diagnosis of cardiac transthyretin amyloidosis. Circulation. 2016;133(24):2404–12 **Seminal paper assessing utility of technetium-labeled radiotracers for non-biopsy diagnosis of ATTR cardiac amyloidosis.**
4. Falk RH, Plehn JF, Deering T, Schick EC Jr, Boinay P, Rubinow A, et al. Sensitivity and specificity of the echocardiographic features of cardiac amyloidosis. Am J Cardiol. 1987;59(5):418–22.
5. Alashi A, Desai RM, Khullar T, Hodges K, Rodriguez ER, Tan C, et al. Different histopathologic diagnoses in patients with clinically diagnosed hypertrophic cardiomyopathy after surgical myectomy. Circulation. 2019;140(4):344–6.
6. Falk RH, Quarta CC, Dorbala S. How to image cardiac amyloidosis. Circ Cardiovasc Imaging. 2014;7(3):552–62.
7. Damy T, Jaccard A, Guellich A, Lavergne D, Galat A, Deux JF, et al. Identification of prognostic markers in transthyretin and AL cardiac amyloidosis. Amyloid. 2016;23(3):194–202.
8. Martinez-Naharro A, Treibel TA, Abdel-Gadir A, Bulluck H, Zumbo G, Knight DS, et al. Magnetic resonance in transthyretin cardiac amyloidosis. J Am Coll Cardiol. 2017;70(4):466–77.
9. Feng D, Syed IS, Martinez M, Oh JK, Jaffe AS, Grogan M, et al. Intracardiac thrombosis and anticoagulation therapy in cardiac amyloidosis. Circulation. 2009;119(18):2490–7.
10. Modesto KM, Dispenzieri A, Cauduro SA, Lacy M, Khandheria BK, Pellikka PA, et al. Left atrial myopathy in cardiac amyloidosis: implications of novel echocardiographic techniques. Eur Heart J. 2005;26(2):173–9.
11. Falk RH, Alexander KM, Liao R, Dorbala S. AL (light-chain) cardiac amyloidosis: a review of diagnosis and therapy. J Am Coll Cardiol. 2016;68(12):1323–41.
12. Koyama J, Ray-Sequin PA, Falk RH. Longitudinal myocardial function assessed by tissue velocity, strain, and strain rate tissue Doppler echocardiography in patients with AL (primary) cardiac amyloidosis. Circulation. 2003;107(19):2446–52.
13.• Knight DS, Zumbo G, Barcella W, Steeden JA, Muthurangu V, Martinez-Naharro A, et al. Cardiac structural and functional consequences of amyloid deposition by cardiac magnetic resonance and echocardiography and their prognostic roles. JACC Cardiovasc Imaging. 2019;12(5):823–33 **Study demonstrating prognostic roles of echo and CMR parameters, which also describes the functional and structural cardiac abnormalities that occur across a spectrum of cardiac amyloid burden in AL and ATTR cardiac amyloidosis, as measured by ECV.**
14. Phelan D, Collier P, Thavendiranathan P, Popovic ZB, Hanna M, Plana JC, et al. Relative apical sparing of longitudinal strain using two-dimensional speckle-tracking echocardiography is both sensitive and specific for the diagnosis of cardiac amyloidosis. Heart. 2012;98(19):1442–8.
15. Liu D, Hu K, Niemann M, Herrmann S, Cikes M, Stork S, et al. Effect of combined systolic and diastolic functional parameter assessment for differentiation of cardiac amyloidosis from other causes of concentric left ventricular hypertrophy. Circ Cardiovasc Imaging. 2013;6(6):1066–72.
16.• Pagourelias ED, Mirea O, Duchenne J, Van Cleemput J, Delforge M, Bogaert J, et al. Echo parameters for differential diagnosis in cardiac amyloidosis: a head-to-head comparison of deformation and nondeformation parameters. Circ Cardiovasc Imaging. 2017;10(3):e005588 **Compared the diagnostic accuracy of various deformation and conventional echo parameters in differentiating CA from other hypertrophic substrates.**
17. Cueto-Garcia L, Reeder GS, Kyle RA, Wood DL, Seward JB, Naessens J, et al. Echocardiographic findings in systemic amyloidosis: spectrum of cardiac involvement and relation to survival. J Am Coll Cardiol. 1985;6(4):737–43.
18. Bodez D, Ternacle J, Guellich A, Galat A, Lim P, Radu C, et al. Prognostic value of right ventricular systolic function in cardiac amyloidosis. Amyloid. 2016;23(3):158–67.
19. Mohty D, Pibarot P, Dumesnil JG, Darodes N, Lavergne D, Echahidi N, et al. Left atrial size is an independent predictor of overall survival in patients with primary systemic amyloidosis. Arch Cardiovasc Dis. 2011;104(12):611–8.
20. Klein AL, Hatle LK, Taliercio CP, Oh JK, Kyle RA, Gertz MA, et al. Prognostic significance of Doppler measures of diastolic function in cardiac amyloidosis. A Doppler echocardiography study. Circulation. 1991;83(3):808–16.
21. Barros-Gomes S, Williams B, Nhola LF, Grogan M, Maalouf JF, Dispenzieri A, et al. Prognosis of light chain amyloidosis with preserved LVEF: added value of 2D speckle-tracking echocardiography to the current prognostic staging system. JACC Cardiovasc Imaging. 2017;10(4):398–407.
22. Maceira AM, Joshi J, Prasad SK, Moon JC, Perugini E, Harding I, et al. Cardiovascular magnetic resonance in cardiac amyloidosis. Circulation. 2005;111(2):186–93.
23. White JA, Kim HW, Shah D, Fine N, Kim KY, Wendell DC, et al. CMR imaging with rapid visual T1 assessment predicts mortality in

patients suspected of cardiac amyloidosis. JACC Cardiovasc Imaging. 2014;7(2):143–56.
24. Fontana M, Pica S, Reant P, Abdel-Gadir A, Treibel TA, Banypersad SM, et al. Prognostic value of late gadolinium enhancement cardiovascular magnetic resonance in cardiac amyloidosis. Circulation. 2015;132(16):1570–9.
25. Kim RJ, Chen EL, Lima JA, Judd RM. Myocardial Gd-DTPA kinetics determine MRI contrast enhancement and reflect the extent and severity of myocardial injury after acute reperfused infarction. Circulation. 1996;94(12):3318–26.
26. Syed IS, Glockner JF, Feng D, Araoz PA, Martinez MW, Edwards WD, et al. Role of cardiac magnetic resonance imaging in the detection of cardiac amyloidosis. JACC Cardiovasc Imaging. 2010;3(2):155–64.
27. Dungu JN, Valencia O, Pinney JH, Gibbs SD, Rowczenio D, Gilbertson JA, et al. CMR-based differentiation of AL and ATTR cardiac amyloidosis. JACC Cardiovasc Imaging. 2014;7(2):133–42.
28. Cuddy SAM, Bravo PE, Falk RH, El-Sady S, Kijewski MF, Park MA, et al. Improved Quantification of cardiac amyloid burden in systemic light chain amyloidosis: redefining early disease? JACC Cardiovasc Imaging. 2020;13(6):1325–36.
29. Dorbala S, Vangala D, Bruyere J Jr, Quarta C, Kruger J, Padera R, et al. Coronary microvascular dysfunction is related to abnormalities in myocardial structure and function in cardiac amyloidosis. JACC Heart Fail. 2014;2(4):358–67.
30. Ferreira VM, Piechnik SK, Dall'Armellina E, Karamitsos TD, Francis JM, Choudhury RP, et al. Non-contrast T1-mapping detects acute myocardial edema with high diagnostic accuracy: a comparison to T2-weighted cardiovascular magnetic resonance. J Cardiovasc Magn Reson. 2012;14:42.
31. Dass S, Suttie JJ, Piechnik SK, Ferreira VM, Holloway CJ, Banerjee R, et al. Myocardial tissue characterization using magnetic resonance noncontrast t1 mapping in hypertrophic and dilated cardiomyopathy. Circ Cardiovasc Imaging. 2012;5(6):726–33.
32. Fontana M, Banypersad SM, Treibel TA, Maestrini V, Sado DM, White SK, et al. Native T1 mapping in transthyretin amyloidosis. JACC Cardiovasc Imaging. 2014;7(2):157–65.
33. Karamitsos TD, Piechnik SK, Banypersad SM, Fontana M, Ntusi NB, Ferreira VM, et al. Noncontrast T1 mapping for the diagnosis of cardiac amyloidosis. JACC Cardiovasc Imaging. 2013;6(4):488–97.
34. Banypersad SM, Fontana M, Maestrini V, Sado DM, Captur G, Petrie A, et al. T1 mapping and survival in systemic light-chain amyloidosis. Eur Heart J. 2015;36(4):244–51.
35.• Martinez-Naharro A, Kotecha T, Norrington K, Boldrini M, Rezk T, Quarta C, et al. Native T1 and extracellular volume in transthyretin amyloidosis. JACC Cardiovasc Imaging. 2019;12(5):810–9 **This study evaluated the prognostic potential of native myocardial T1 in cardiac transthyretin amyloidosis (ATTR) and compared native T1 with extracellular volume (ECV) in terms of diagnostic accuracy and prognosis.**
36. Messroghli DR, Moon JC, Ferreira VM, Grosse-Wortmann L, He T, Kellman P, et al. Clinical recommendations for cardiovascular magnetic resonance mapping of T1, T2, T2* and extracellular volume: a consensus statement by the Society for Cardiovascular Magnetic Resonance (SCMR) endorsed by the European Association for Cardiovascular Imaging (EACVI). J Cardiovasc Magn Reson. 2017;19(1):75.
37. Banypersad SM, Sado DM, Flett AS, Gibbs SD, Pinney JH, Maestrini V, et al. Quantification of myocardial extracellular volume fraction in systemic AL amyloidosis: an equilibrium contrast cardiovascular magnetic resonance study. Circ Cardiovasc Imaging. 2013;6(1):34–9.
38. Mongeon FP, Jerosch-Herold M, Coelho-Filho OR, Blankstein R, Falk RH, Kwong RY. Quantification of extracellular matrix expansion by CMR in infiltrative heart disease. JACC Cardiovasc Imaging. 2012;5(9):897–907.
39. Kotecha T, Martinez-Naharro A, Treibel TA, Francis R, Nordin S, Abdel-Gadir A, et al. Myocardial edema and prognosis in amyloidosis. J Am Coll Cardiol. 2018;71(25):2919–31.
40.• Martinez-Naharro A, Abdel-Gadir A, Treibel TA, Zumbo G, Knight DS, Rosmini S, et al. CMR-verified regression of cardiac AL amyloid after chemotherapy. JACC Cardiovasc Imaging. 2018;11(1):152–4 **Small longitudinal study showing decrease in amyloid burden by ECV.**
41. Fontana M, Martinez-Naharro A, Chacko L, Rowczenio D, Gilbertson JA, Whelan CJ, et al. Reduction in CMR derived extracellular volume with patisiran indicates cardiac amyloid regression. JACC Cardiovasc Imaging. 2021;14(1):189–99.
42. Stats MA, Stone JR. Varying levels of small microcalcifications and macrophages in ATTR and AL cardiac amyloidosis: implications for utilizing nuclear medicine studies to subtype amyloidosis. Cardiovasc Pathol. 2016;25(5):413–7.
43. Perugini E, Guidalotti PL, Salvi F, Cooke RM, Pettinato C, Riva L, et al. Noninvasive etiologic diagnosis of cardiac amyloidosis using 99mTc-3,3-diphosphono-1,2-propanodicarboxylic acid scintigraphy. J Am Coll Cardiol. 2005;46(6):1076–84.
44.•• Dorbala S, Ando Y, Bokhari S, Dispenzieri A, Falk RH, Ferrari VA, et al. ASNC/AHA/ASE/EANM/HFSA/ISA/SCMR/SNMMI Expert Consensus Recommendations for multimodality imaging in cardiac amyloidosis: part 1 of 2-evidence base and standardized methods of imaging. J Card Fail. 2019;25(11):e1–e39 **Expert Consensus Recommendations for multimodality imaging of amyloidosis, with a comprehensive review of literature in the field.**
45. Hutt DF, Quigley AM, Page J, Hall ML, Burniston M, Gopaul D, et al. Utility and limitations of 3,3-diphosphono-1,2-propanodicarboxylic acid scintigraphy in systemic amyloidosis. Eur Heart J Cardiovasc Imaging. 2014;15(11):1289–98.
46. Bokhari S, Castano A, Pozniakoff T, Deslisle S, Latif F, Maurer MS. (99m)Tc-pyrophosphate scintigraphy for differentiating light-chain cardiac amyloidosis from the transthyretin-related familial and senile cardiac amyloidoses. Circ Cardiovasc Imaging. 2013;6(2):195–201.
47. Castano A, Haq M, Narotsky DL, Goldsmith J, Weinberg RL, Morgenstern R, et al. Multicenter study of planar technetium 99m pyrophosphate cardiac imaging: predicting survival for patients with ATTR cardiac amyloidosis. JAMA Cardiol. 2016;1(8):880–9.
48.• Hanna M, Ruberg FL, Maurer MS, Dispenzieri A, Dorbala S, Falk RH, et al. Cardiac scintigraphy with technetium-99m-labeled bone-seeking tracers for suspected amyloidosis: JACC review topic of the week. J Am Coll Cardiol. 2020;75(22):2851–62 **Important review highlighting common errors in scan acquisition and interpretation that can lead to misdiagnosis of ATTR.**
49. Dewanjee MK, Kahn PC. Mechanism of localization of 99mTc-labeled pyrophosphate and tetracycline in infarcted myocardium. J Nucl Med. 1976;17(7):639–46.
50. Azevedo Coutinho MC, Cortez-Dias N, Cantinho G, Goncalves S, Menezes MN, Guimaraes T, et al. The sensitivity of DPD scintigraphy to detect transthyretin cardiac amyloidosis in V30M mutation depends on the phenotypic expression of the disease. Amyloid. 2020;27(3):174–83.
51. Mockelind S, Axelsson J, Pilebro B, Lindqvist P, Suhr OB, Sundstrom T. Quantification of cardiac amyloid with [(18)F]Flutemetamol in patients with V30M hereditary transthyretin amyloidosis. Amyloid. 2020;27(3):191–9.
52. Chang ICY, Bois JP, Bois MC, Maleszewski JJ, Johnson GB, Grogan M. Hydroxychloroquine-mediated cardiotoxicity with a false-positive ^{99m}technetium-labeled pyrophosphate scan for transthyretin-related cardiac amyloidosis. Circ Cardiovasc

Imaging. 2018;11(1):e007059. https://doi.org/10.1161/CIRCIMAGING.117.007059.

53.• Scully PR, Patel KP, Treibel TA, Thornton GD, Hughes RK, Chadalavada S, et al. Prevalence and outcome of dual aortic stenosis and cardiac amyloid pathology in patients referred for transcatheter aortic valve implantation. Eur Heart J. 2020;41(29):2759–67 **Study showing prevalence of disease in AS cohort.**

54. Sperry BW, Reyes BA, Ikram A, Donnelly JP, Phelan D, Jaber WA, et al. Tenosynovial and cardiac amyloidosis in patients undergoing carpal tunnel release. J Am Coll Cardiol. 2018;72(17):2040–50.

55. Law WP, Wang WY, Moore PT, Mollee PN, Ng AC. Cardiac amyloid imaging with 18F-florbetaben PET: a pilot study. J Nucl Med. 2016;57(11):1733–9.

56. Dorbala S, Vangala D, Semer J, Strader C, Bruyere JR Jr, Di Carli MF, et al. Imaging cardiac amyloidosis: a pilot study using (1)(8)F-florbetapir positron emission tomography. Eur J Nucl Med Mol Imaging. 2014;41(9):1652–62.

57. Antoni G, Lubberink M, Estrada S, Axelsson J, Carlson K, Lindsjo L, et al. In vivo visualization of amyloid deposits in the heart with 11C-PIB and PET. J Nucl Med. 2013;54(2):213–20.

58. Gallegos C, Miller EJ. Advances in PET-based cardiac amyloid radiotracers. Curr Cardiol Rep. 2020;22(6):40.

59. Castano A, DeLuca A, Weinberg R, Pozniakoff T, Blaner WS, Pirmohamed A, et al. Serial scanning with technetium pyrophosphate ((99m)Tc-PYP) in advanced ATTR cardiac amyloidosis. J Nucl Cardiol. 2016;23(6):1355–63.

60. Rapezzi C, Merlini G, Quarta CC, Riva L, Longhi S, Leone O, et al. Systemic cardiac amyloidoses: disease profiles and clinical courses of the 3 main types. Circulation. 2009;120(13):1203–12.

61. Carroll JD, Gaasch WH, McAdam KP. Amyloid cardiomyopathy: characterization by a distinctive voltage/mass relation. Am J Cardiol. 1982;49(1):9–13.

62. Helder MR, Schaff HV, Nishimura RA, Gersh BJ, Dearani JA, Ommen SR, et al. Impact of incidental amyloidosis on the prognosis of patients with hypertrophic cardiomyopathy undergoing septal myectomy for left ventricular outflow tract obstruction. Am J Cardiol. 2014;114(9):1396–9.